Carbohydrate Polymers 74 (2008) 685–690

Contents lists available at ScienceDirect

Carbohydrate Polymers

journal homepage: www.elsevier.com/locate/carbpol

Aggregation behavior of sodium alginate with cucurbit[6]uril in aqueous solution

Xiaoling Huang, Yebang Tan *, Qifeng Zhou, Yuexia Wang, Yuju Che

The Key Laboratory of Colloid and Interface Chemistry, School of Chemistry and Chemical Engineering, Shandong University, Ministry of Education, Jinan, 250100, PR China

ARTICLE INFO

Article history:
Received 7 September 2007
Received in revised form 1 February 2008
Accepted 23 April 2008
Available online 29 April 2008

Keywords:
Alginate
Cucurbit[6]uril
Aggregation behavior

ABSTRACT

The interaction between the polysaccharide alginate and cucurbit[6]uril (CB[6]) in aqueous solution has been investigated by static fluorescence spectroscopy, dynamic light scattering, transmission electron microscopy, circular dichroism (CD) and zeta potential. Results showed that the interactions between the alginate and the CB[6] lead to the formation of micelle-like nanometer-sized aggregates due to electrostatic interaction and iondipole interaction. The size of aggregates depends on the concentration of alginate. In our experiment, only when the concentration of sodium alginate was 0.05 wt%, were uniform micelle-like aggregates achieved. With the increase in the concentration of alginate, the size of aggregates increased. When the concentration of alginate was above 0.2 wt%, the aggregates became precipitates after 48 h of storage at room temperature. As the concentration of sodium alginate was raised to about 0.5 wt%, gelation appeared. At low concentrations of alginate (around 0.01 wt%), few micelles-like nanometer-sized aggregates were observed. The aggregation also depends on the mole ratio of CB[6]/carboxyl in alginate. Isolated micelle-like aggregates prevailed at low stoichiometric mole ratio of CB[6]/carboxyl in alginate and the clusters were predominant with increasing the mole ratio of CB[6]/carboxyl in alginate due to the decrease of charges at the surface of the micelle-like aggregates.

1. Introduction

Polymer nanometer aggregates has recently attracted much interest because of not only their unique morphological behaviors, but also their potential applications in biological and medical areas such as drug delivery, encapsulation and gene therapy. Therefore, the use of polymer to form micelles or micelle-like aggregates in an aqueous phase has been growing (Lee, Cho, & Cho, 2004; Lee, Huang, & Lee, 2006).

Alginates are biocompatible unbranched binary copolymers of (1–4)-linked residues of β-D-mannuronic (M) and α-L-guluronic (G) acids as show in Fig. 1a (Draget, Stokke, Yuguchi, Urakawa, & Kajiwara, 2003). Alginate is a valuable material used to make microcapsules for drug delivery and immobilization of biocatalysts, coatings for medical implants, food thickeners, textile print thickeners, and a wide variety of other applications where its unique barrier, ion chelating, and biocompatible properties are useful (Huaitian, Anna-Lena, Knudsen, & Nyström, 2004; Orive, Ponce, & Hernandez, 2002).

Cucurbit[6]uril (CB[6]) has received much interest in the last two decades as a synthetic receptor and has been used in inclusion catalysis, interlocked architectures and functional molecular devices (Krasia, & Steinke, 2002). CB[6] is composed of six symmetrically arranged glycoluril units covalently linked by 12 methylene bridges to form a rigid, annular, hollow cavity with two highly polar carbonyl openings (see structure in Fig. 1b). The polar carbonyl groups at the portals and the hydrophobic cavity allow the cavity to form stable host–guest complexes with small molecules (Kim et al., 2007). Taking advantage of this fact, various mechanically interlocked molecules including rotaxanes and (pseudo)polyrotaxanes have been synthesized by Kim (Choi, Lee, Ko, & Kim, 2002; Dybtsev, Chun, Yoon, Kim, & Kim, 2004; Jeon et al., 2003; Kim, Kim, Lee, Ko, & Kim, 2004; Kim et al., 2003; Lee, Heo, & Kim, 2000; Lee, Kim, & Kim, 2001; Tan, Choi, Lee, Ko, & Kim, 2002; Whang, Park, Heo, & Kim, 1998) and others (Buschmann, Jansen, & Schollmeyer, 2000; Meschke, Hoecker, & Buschman, 1999; Nesch-hke, Buschmann, & Schollmeyer, 1998). Some side-chain (pseudo)polyrotaxanes containing CB[6] as a molecular bead have been also reported by us (Hou, Tan, & Zhou, 2005, 2006; Hou, Tan, Kim, & Zhou, 2006).

Based on this work, we investigated the weak interactions between polysaccharide alginate and CB[6] leading to CB[6]-mediated molecular aggregates. The CB[6] can complex to the carboxyl groups in sodium alginate chains, which leads to the aggregation of micelle-like nanometer-sized aggregates. These novel micelle-like aggregates were physicochemically characterized by fluorescence techniques, dynamic light scattering, circular dichroism (CD) and transmission electron microscopy.

* Corresponding author. Tel.: +86 531 88567509; fax: +86 531 88564464.
E-mail address: ybtan@sdu.edu.cn (Y. Tan).

0144-8617/$ - see front matter © 2008 Elsevier Ltd. All rights reserved.
doi:10.1016/j.carbpol.2008.04.030

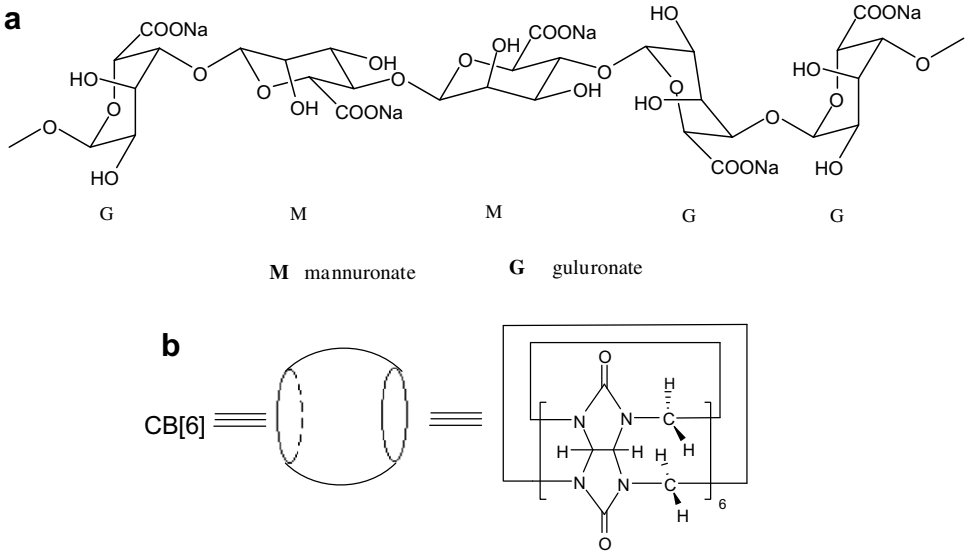

Fig. 1. The structure of (a) sodium alginate and (b) Cucurbit[6]uril (CB[6]).

2. Experimental

2.1. Materials

Sodium alginate was purchased from Tianjin Kermel Stock of China Medicine Company, refined twice by dissolving it in distilled water, filtered, precipitated with ethanol and finally dried in vacuum at 60 °C. The average molecular weight (M_w) of sodium alginate is 2.7×10^5 g/mol calculated using the experimentally determined [η] and the Mark-Houwink equation [η] (mL/g) = 4.84×10^{-3} $M_w^{0.97}$ (Stokke, Draget, Smidsrod, & Yuguchi, 2000). The intrinsic viscosity ([η]; mL/g) of alginate in 0.1 M NaCl is 900 mL/g measured with a capillary viscometry. The ratio of mannuronic acid to guluronic acid (M/G) in alginate was determined by circular dichroism. (M/G = 1.78) (Donati et al., 2003).

Cucurbit[6]uril was prepared according to the literature (Freeman, Mock, & Shih, 1981). Pyrene was purchased from Alfa Aesar analytic reagent company and recrystallized twice from benzene. Sodium chloride was of analytical grade and used as received.

2.2. Preparation of micelle-like aggregates

Sodium alginate was dissolved in ultra pure water under magnetic stirring at room temperature. The desired amount of CB[6] was dissolved in 0.2 mol/L NaCl solution. All the solutions were filtered through a 0.8 μm Millipore filter. Micelle-like aggregates were achieved under magnetic stirring by addition of desired CB[6] solution to alginate solution.

2.3. Fluorescence measurements

Steady-state fluorescent measurements were performed on a Hitachi F-4500 fluorescence spectrophotometer (Tokyo, Japan) at room temperature using 1.0 cm quartz cells. Pyrene was chosen as the fluorescent probe to study the aggregation of the blend solutions of CB[6] and alginate. Pyrene was dissolved in 10 mL of the blend solutions. Pyrene was excited at 335 nm, and emission spectra were recorded from 350 to 450 nm with excitation and emission slit widths of 2.5 nm. Intensities, I_1 and I_3, were taken from the emission intensities at 373 and 384 nm, respectively.

2.4. Circular dichroism(CD)

Circular dichroism measurements were performed on a Jasco J-810 spectropolarimeter (Jasco Corporation, Tokyo, Japan). A flat-faced quartz sample cell of 10 mm optical path length was used and the following set up maintained: bandwidth, 2 nm; time constant, 2 s; scan rate, 20 nm/min. Three spectra were averaged for each sample. All experiments were performed at 25 °C.

2.5. Dynamic light scattering

Dynamic light scattering (DLS) was conducted to measure the sizes and the distribution of hydrodynamic radius of micelle-like aggregates in the blend solutions of CB[6] and alginate. The measurements were performed on the multi-detector light scattering unit (DAWN HELEOS, Wyatt Technology Corporation, US). All dynamic light scattering were measured three times at 25 °C.

2.6. Transmission electron microscopy

Aggregates morphology was confirmed by transmission electron microscopy (TEM) (JEMXC, Japan). The samples were immobilized on copper grids covered with carbon and stained with phosphotungstic acid. The specimens were dried at room temperature before examination.

2.7. Zeta potential and pH value measurement

The pH measurements were performed on a pHS-3 C. The zeta potential of the micelle-like aggregates was achieved with Zetasizer 3000 (MALVERN Instruments, Britain). The average values of zeta potential and pH value were obtained from three repetitions.

3. Results and discussion

3.1. Micropolarity

The fluorescence of pyrene is known to be sensitive to changes in the microenvironment. When the hydrophobic microdomain is formed in an aqueous phase, pyrene molecules are preferentially located within or close to the hydrophobic microdomain. The photophysical characteristics of pyrene molecules in a hydropho-

bic surrounding differ noticeably from those in an aqueous phase. The intensity ratio of the first and the third major vibrational peaks in pyrene's fluorescence spectrum (I_1/I_3) is often used as a measure of the polarity of the microenvironment (Wu et al., 2007).

Fig. 2 shows the variation of I_1/I_3 values as a function of the mole ratio of CB[6]/carboxyl in alginate at different alginate concentrations. In this work, the stoichiometric mole ratio CB[6]/carboxyl in alginate is determined by f. The I_1/I_3 values of the mixture solutions of the CB[6] and the 0.01 wt% alginate at different f values have negligible variation as shown in curve a of Fig. 2, which are almost the same as that of the pure 0.01 wt% alginate solution. These results suggest that the polarities of the microenvironments with and without CB[6] are similar at 0.01 wt% alginate. Evidently, there are few micelle-like aggregates formed in the system of 0.01 wt% alginate. The I_1/I_3 values of the blend solutions of the CB[6] and the 0.05 wt% alginate show rapid decay from 1.65 to 1.40 with the increase of f value from 0.090 to 0.157 as shown in curve b of Fig. 2. The sharp decrease of I_1/I_3 values is due to the formation of micelle-like aggregates, which leads to the formation of hydrophobic microdomain. The curve c of Fig. 2 shows the I_1/I_3 values as a function of f values at 0.09 wt% alginate system. At low f values, the I_1/I_3 values of the blend solutions of CB[6] and 0.09 wt% alginate decrease rapidly with the increase of f value, and are lower than that of the 0.05 wt% alginate system. There is no apparent transition in the entire f value we studied. This phenomenon is ascribed to the formation of micelle-like aggregates at low f value in the 0.09 wt% alginate system.

3.2. Circular dichroism studies (CD)

Fig. 3 is the CD spectra of pure 0.05 wt% alginate solution and the mixture of CB[6] and 0.05 wt% alginate solutions. The CD spectra of pure 0.05 wt% alginate solution exhibit a negative band near 215 nm in circular dichroism, which may assign to the carboxylate $n\rightarrow\pi^*$ transition (Sreeram, Yamini Shrivastava, & Nair, 2004). With the adding of CB[6], a minor blue shift of $n\rightarrow\pi^*$ transition with decreasing ellipticity at around 215 nm is observed. It is proposed that such a decrease in the ellipticity and a minor blue shift of the $n\rightarrow\pi^*$ transition reflects the binding of CB[6] to carboxylate inducing the changes of the microenvironment around the carboxyl site (Donati et al., 2003).

3.3. Dynamic light scattering (DLS)

DLS measurements were conducted to characterize the sizes of the micelle-like aggregates. Fig. 4 shows the distributions of the R_h

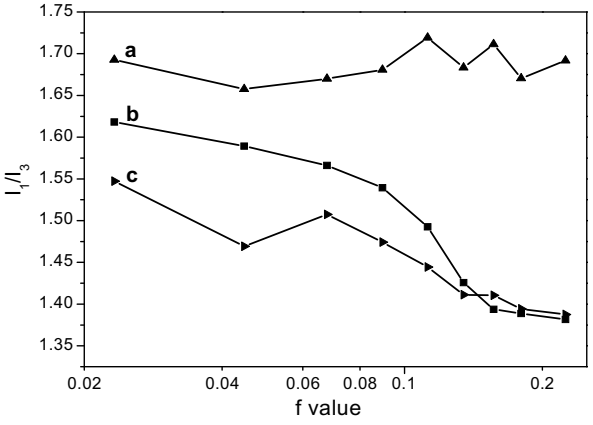

Fig. 2. Value of I_1/I_3 as a function of f value in the blend solutions of CB[6] and alginate (the concentration of alginate: a, 0.01 wt%; b, 0.05 wt%; c, 0.09 wt%).

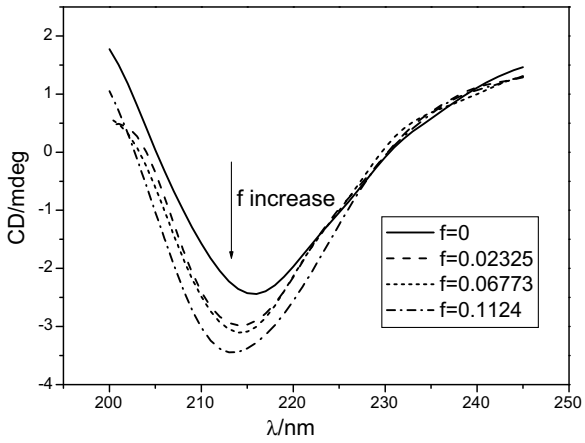

Fig. 3. CD spectra of 0.05 wt% alginate system at different f values.

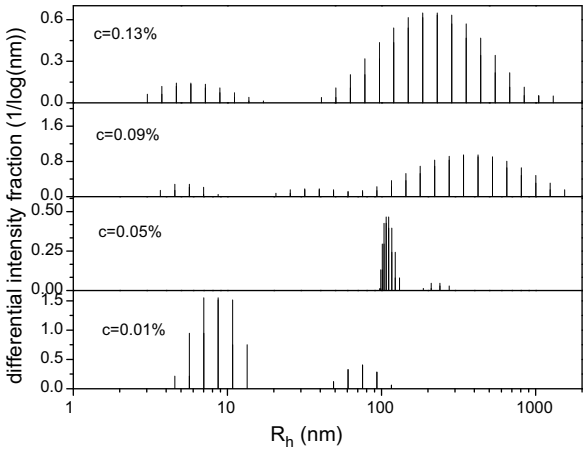

Fig. 4. Differential intensity fraction of hydrodynamic radius of aggregates at f = 0.09 at different concentration (c was the concentration of alginate).

of the aggregates of the CB[6] and the alginate solutions at f = 0.09 at different concentration of alginate. It can be seen that the concentration of alginate plays an important role in controlling the size of aggregates. At 0.09 wt% and 0.13 wt% alginate, the R_h of the aggregates was considerably higher than that of the 0.01 wt% and 0.05 wt% alginate system. For 0.09 wt% alginate and 0.13 wt% alginate system, very wide distributed aggregates were observed in our experiments. The sizes of aggregates fluctuate from 1000 nm to 10 nm. With the increasing the concentration of sodium alginate to 0.2 wt%, the aggregates became precipitates after 48 h of storage at room temperature. With further increasing the concentration of alginate to 0.5 wt%, a gel of alginate was obtained. When the concentration of sodium alginate decreased to 0.01 wt%, the scatter intensity of the aggregates with sizes in 100 nm was very low. This means that the number of amphiphilic aggregates are small in the blend solutions of CB[6] and 0.01 wt% alginate. In our experiment, the optimum concentration of sodium alginate was 0.05 wt%, at which the uniform micelle-like aggregates were obtained.

The typical distributions of the hydrodynamic radius of the blend solutions of CB[6] and 0.05 wt% alginate at different f values are shown in Fig. 5. Bimodal distribution of R_h of the blend solutions is observed. Considering that one CB[6] is able to connect with two carboxylates in alginate which may located in one isolated particle or two particles. In the latter case, the alginate can bridge particles forming a cluster. Therefore, in the final solutions,

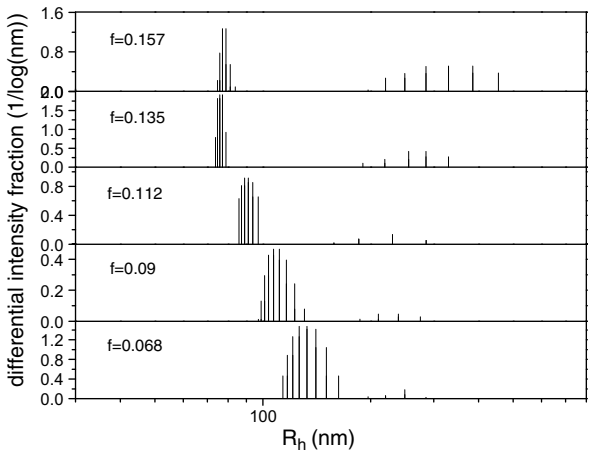

Fig. 5. Differential intensity fraction of hydrodynamic radius of aggregates at different f value at the concentration of alginate is 0.05 wt%.

isolated particles and clusters may coexist. In Fig. 5, the large peak located at about 100 nm can be attributed to the isolated particles. The small peak ranging from 200 to 400 nm should be associated with the clusters. With the increase of f values, the proportion of clusters increased.

The average R_h and zeta potential of micelle-like aggregates as a function of f values are shown in Fig. 6. It can be seen that the average R_h decreases initially with the increase of the f value and reaches a minimum value, 76.8 nm, at the calculated $f = 0.135$ (curve b of Fig. 6). Progressively increasing the f values results in the increase of the R_h of micelle-like aggregates.

It is apparent that the addition of CB[6] can interact with the dissociated carboxyl groups on alginate chains due to electrostatic interaction and iondipole interaction, leading to the local physical cross-linking, which makes alginate lose its hydrophilicity to some extent. The occurrence of physical cross-link segments in alginate chains drives the formation of amphiphilic aggregates.

The increasing of f values makes the zeta potential decrease as shown in curve a of Fig. 6, namely, the charges at the surface of the aggregates decrease. With the decrease of the surface charges, the electrostatic repulsions among the different particles are not strong enough; some of the particles may move closer making it easier for the formation of clusters, resulting in the increase of the average size of aggregates with the increase of the number of clusters. When the f values reach 0.157, the peak centered at 300 nm is dominant as shown in Fig. 5.

It is known that the partial protonation of dissociated carboxyl groups in the alginate can form amphiphilic aggregates (Yi et al., 2005). The pH value influences the degree of protonation of dissociated carboxyl groups on alginate chains. In order to suppress the interference of protonation of dissociated carboxyl groups on the aggregation behavior, we study the pH value in the blend solutions of CB[6] and alginate. Fig. 7 shows the pH value of the blend solutions of 0.05 wt% alginate and CB[6] in different f values. The result means that there is no apparent change by adding the CB[6]. So we can conclude that the aggregation behavior in the blend solutions of CB[6] and alginate occurred due to the interaction between CB[6] and sodium alginate.

3.4. Transmission electron microscopy (TEM)

Morphologies of micelle-like aggregates were observed by transmission electron microscopy as shown in Fig. 8. Fig. 8a displays the micrographs of aggregates of 0.09 wt% alginate at $f = 0.09$. It is noticeable that a large number of different size particles were observed. The wide size distribution of the aggregates of 0.09 wt% alginate is also visualized by DLS.

Fig. 8b shows the TEM image of aggregates of 0.05 wt% alginate at $f = 0.09$. The core and shell of the aggregates are clearly observed. The radius of particles is about 150 nm. Based on the zeta potential of aggregates (−37.943 mV), we come to the conclusion that micelle-like core-shell aggregates with the physical cross-link segments as the core and the dissociated carboxyl in alginate as the shell were formed. In the shell of the isolated particles, dissociated carboxyl segments may form loop and swelling ends, both of which can stabilize the particles.

Fig. 8c shows the TEM of particles of 0.05 wt% alginate solution at $f = 0.135$. It can be seen that the structure of the micelle-like aggregates become considerable compact and the swollen shell almost disappeared. With the increase of f value, the hydrophobic crosslink segments increase and the hydrophilic segments decrease, which makes the particles compact, resulting in the substantial decrease in the size of the alginates aggregates. The results are in good agreement with DLS data as shown in Fig. 6b.

Fig. 8d shows the TEM of 0.05 wt% alginate solution at $f = 0.157$, the main feature of the micrograph is the coexistence of isolated particles and clusters with multicore structure as indicated by arrow one and arrow two, respectively. The results are in good agreement with DLS data as shown in Fig. 5. Thus, we can conclude that

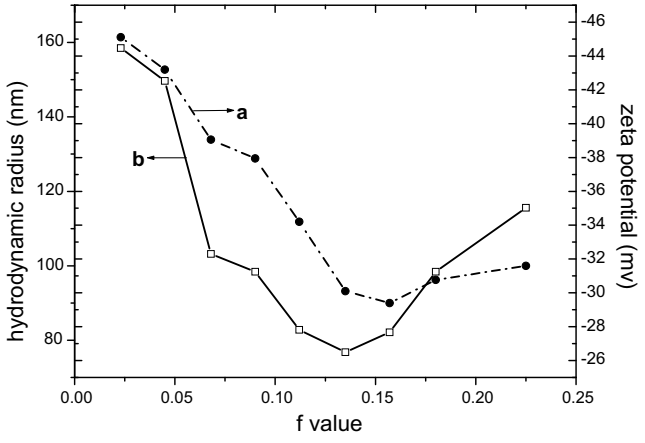

Fig. 6. Average R_h and zeta potential of micelle-like aggregates as a function of f value at the concentration of alginate is 0.05 wt%: (a) zeta potential; (b) hydrodynamic radius.

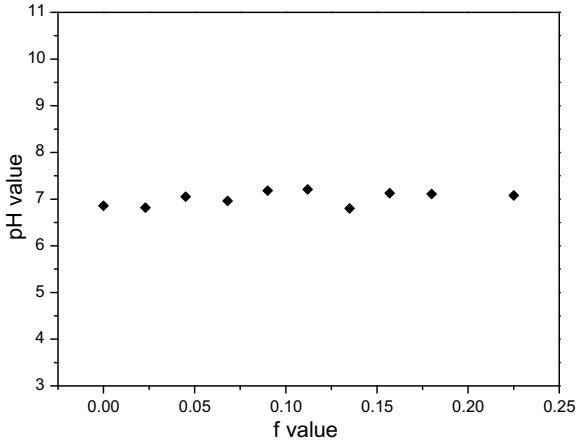

Fig. 7. pH value of the blend solutions of 0.05 wt% alginate and CB[6] as a function of f value.

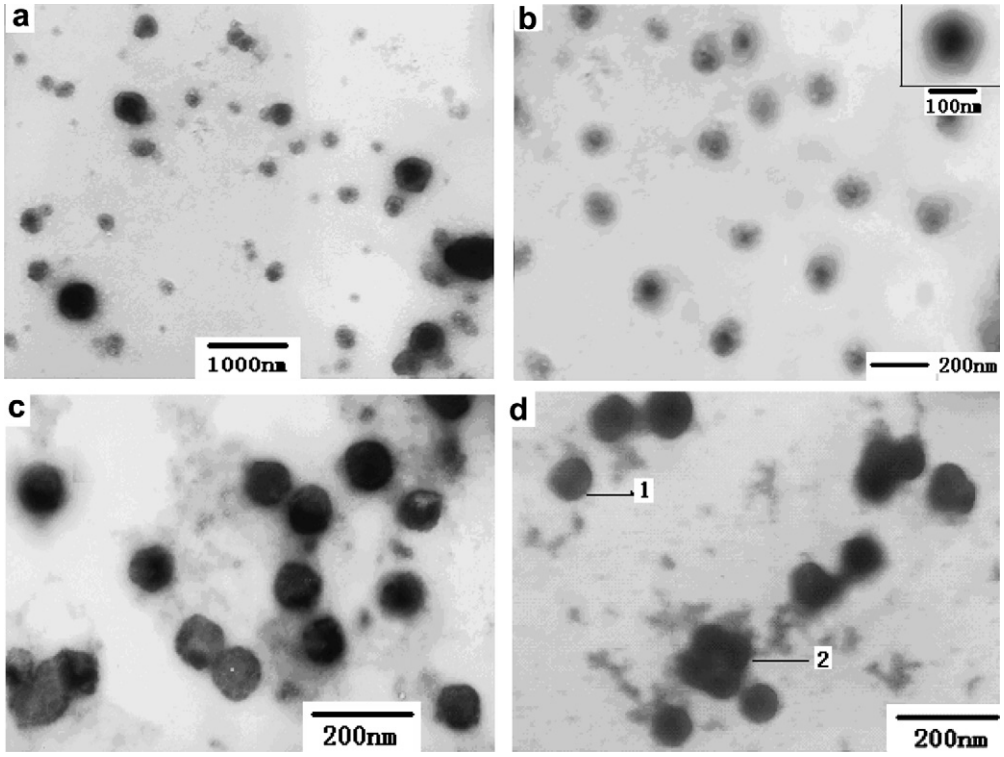

Fig. 8. The morphology of micelle-like aggregates by TEM (a) the concentration of alginate is 0.09 wt%, $f = 0.09$; (b) the concentration of alginate is 0.05 wt%, $f = 0.09$; (c) the concentration of alginate is 0.05 wt%, $f = 0.135$; (d) the concentration of alginate is 0.05 , $f = 0.157$.

the increase of aggregates size when the f value increases from 0.135 to 0.225 may be the increase of cluster.

The radius of particles observed by TEM is smaller than its diameter obtained by the DLS experiment. The radius of aggregates obtained from the DLS experiment reflect the hydrodynamic radius of micelle-like aggregates that are swelled by water molecules, whereas the size of particles observed by TEM shows that of dried particles (Lee et al., 2004). Therefore, an increase in the aggregates size obtained from DLS compared to that of TEM is assumed to be caused by the hydration of the shell portion of particles.

3.5. Possible modes of micelle-like aggregates

Based on all the results described above, a schematic representation for the isolated particles and clusters is suggested as shown in Fig. 9. For isolated particles, CB[6] cross-linked alginate segment form core surrounded by the solvated ionized alginate segments and ion sites are located at the interface which can stabilize the particles. The clusters consist of compact micelle-like aggregates domains linked by bridges.

4. Conclusion

In this study, we investigated the aggregation behaviors in aqueous between sodium alginate and CB[6]. The carboxyl groups in alginate chains can complex to CB[6], which lead to the formation of micelle-like nanometer-sized polymer aggregates. The size of the aggregates was affected by the concentration of alginate and f value. We found that the optimum concentration of sodium alginate was 0.05 wt%. The uniform particles were obtained in the 0.05 wt% alginate solution. DLS and TEM results both showed that isolated particles and clusters coexist in the blend solutions of CB[6] and alginate. At low f value, isolated aggregates were the ma-

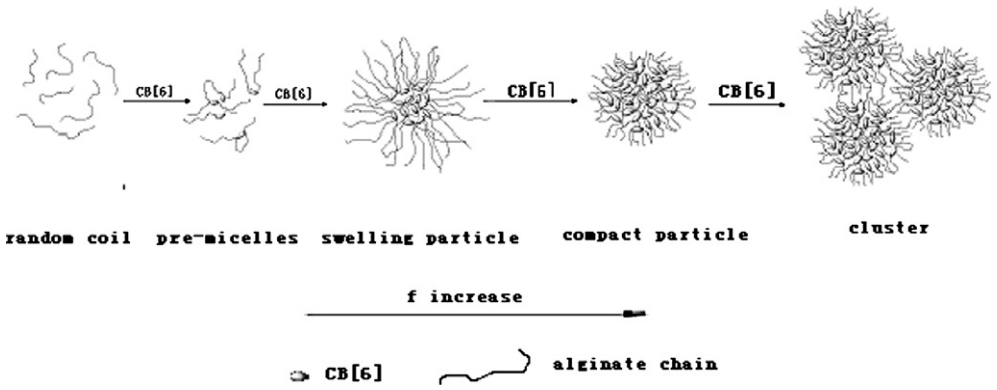

Fig. 9. Schematic representation of the simplified model formation of micelle-like aggregates and clusters by CB[6] and alginate in solution.

jor proportion, whereas at high *f* value, the number of clusters increased a lot due to the decrease of surface charge of particles.

Acknowledgements

The Project was sponsored by the Scientific Research Foundation for the Returned Overseas Chinese Scholars, State Education Ministry (202247) and the Scientific Research Foundation of Key Laboratory of Colloid and Interface Chemistry, Shandong University, Ministry of Education(200610).

References

Buschmann, H. J., Jansen, K., & Schollmeyer, E. (2000). Cucurbituril as host molecule for the complexation of aliphatic alcohols, acids and nitriles in aqueous solution. *Thermochimica Acta, 346*, 33–36.

Choi, S. W., Lee, J. W., Ko, Y. H., & Kim, K. (2002). Pseudopolyrotaxanes made to order: Cucurbituril threaded on polyviologen. *Macromolecules, 35*, 3526–3531.

Donati, I., Gamini, A., Skjak-Bræk, G., Vetere, A., Campa, C., Coslovi, A., et al. (2003). Determination of the diadic composition of alginate by means of circular dichroism: A fast and accurate improved method. *Carbohydrate Research, 338*, 1139–1142.

Draget, K. I., Stokke, B. T., Yuguchi, Y., Urakawa, H., & Kajiwara, K. (2003). Small-angle X-ray scattering and rheological characterization of alginate gels. 3.alginic acid gels. *Biomacromolecules, 4*, 1661–1668.

Dybtsev, D. N., Chun, H., Yoon, S. H., Kim, D., & Kim, K. (2004). Microporous manganese formate: A simple metal-organic porous material with high framework stability and highly selective gas sorption properties. *Journal of the Chemical Society, 126*, 32–33.

Freeman, W. A., Mock, W. L., & Shih, N. Y. (1981). Cucurbituril. *Journal of the American Chemical Society, 103*, 7367–7368.

Hou, Z., Tan, Y., Kim, K., & Zhou, Q. (2006). Synthesis, characterization and properties of side-chain pseudopolyrotaxanes consisting of cucurbituril[6] and poly-N1-(4-vinylbenzyl)-1,4-diaminobutane dihydrochloride. *Polymer, 47*, 742–750.

Hou, Z., Tan, Y., & Zhou, Q. (2005). Synthesis and characterization of side-chain pesodopolyrotaxanes by supramolecular self-assembly of cucurbituril[6] and poly(4-vinyl-N-n-butypyridinium bromide). *Acta Polymerica Sinica, 4*, 491–495.

Hou, Z., Tan, Y., & Zhou, Q. (2006). Side-chain pseudopolyrotaxanes by threading cucurbituril[6] onto quaternized poly-4-vinylpyridine derivative: Synthesis and properties. *Polymer, 47*, 5267–5274.

Huaitian, B., Anna-Lena, K., Kenneth, K. D., & Nyström, B. (2004). Rheological and structural properties of aqueous alginate during gelation via the ugi multicomponent condensation reaction. *Biomacromolecules, 5*, 1470–1479.

Jeon, W. S., Ziganshina, A. Y., Lee, J. W., Ko, Y. H., Kang, J. K., Lee, C., et al. (2003). A pseudorotaxane-based molecular machine: Reversible formation of a molecular loop driven by electrochemical and photochemical stimuli. *Angewandte Chemie International Edition, 42*, 4097–4100.

Kim, K., Jeon, W. S., Kang, J. K., Lee, J. W., Jon, S. Y., Kim, T., et al. (2003). A pseudorotaxane on gold: Formation of self-assembled monolayers, reversible dethreading and rethreading of the ring, and ion-gating behavior. *Angewandte Chemie International Edition, 42*, 2293–2296.

Kim, K., Kim, D., Lee, J. W., Ko, Y. H., & Kim, K. (2004). Growth of poly(pseudorotaxane) on gold using host-stabilized charge-transfer interaction. *Chemical Communications*, 848–849.

Kim, K., Selvapalam, N., Ko, Y. H., Park, K. M., Kim, D., & Kim, J. (2007). *Functionalized cucurbiturils and their applications*. Chemical Society Reviews.

Krasia, T. C., & Steinke, J. H. G. (2002). Formation of oligotriazoles catalysed by cucurbituril. *Chemical Communications*, 22–23.

Lee, J., Cho, E. C., & Cho, K. (2004). Incorporation and release behavior of hydrophobic drug in functionalized poly(D,L-lactide)-block-poly(ethylene oxide) micelles. *Journal of Controlled Release, 94*, 323–335.

Lee, E., Heo, J., & Kim, K. (2000). A three-dimensional polyrotaxane network. *Angewandte Chemie International Edition, 39*, 2699–2701.

Lee, C.-T., Huang, C.-P., & Lee, Y.-D. (2006). Preparation of amphiphilic poly(L-lactide)-graft-Chondroitin sulfate copolymer self-aggregates and its aggregation behavior. *Biomacromolecules, 7*, 1179–1186.

Lee, J. W., Kim, K., & Kim, K. (2001). A kinetically controlled molecular switch based on bistable [2]rotaxane. *Chemical Communications*, 1042–1043.

Meschke, C., Hoecker, H., & Buschman, H. J. (1999). Polyrotaxanes and pseudopolyrotaxanes of polyamides and cucurbituril. *Polymer, 40*, 945–949.

Neschke, C., Buschmann, H. J., & Schollmeyer, E. (1998). Synthesis of mono-, oligo- and polyamide-cucurbituril rotaxanes. *Macromolecular Rapid Communications, 19*, 59–63.

Orive, G., Ponce, S., & Hernandez, R. M. (2002). Biocompatibility of microcapsules for cell immobilization elaborated with different type of alginates. *Biomaterials, 23*, 3825–3831.

Sreeram, K. J., Yamini Shrivastava, H., & Nair, B. U. (2004). Studies on the nature of interaction of iron(III) with alginates. *Biochimica et Biophysica Acta, 1670*, 121–125.

Stokke, B. T., Draget, K. I., Smidsrod, O., & Yuguchi, Y. (2000). Small-angle X-ray scattering and rheological characterization of alginate gels. 1. Ca-alginate gels. *Macromolecules, 33*, 1853–1863.

Tan, Y. B., Choi, S. W., Lee, J. W., Ko, Y. H., & Kim, K. (2002). Synthesis and characterization of novel side-chain pseudopolyrotaxanes containing cucurbituril. *Macromolecules, 35*, 7161–7165.

Whang, D., Park, K. M., Heo, J., & Kim, K. (1998). Molecular necklace: Quantitative self-assembly of a cyclic oligorotaxane from nine molecules. *Journal of the American Chemical Society, 120*, 4899–4900.

Wu, D., Xu, G., Sun, Y., Zhang, H., Mao, H., & Feng, Y. (2007). Interaction between proteins and cationic gemini surfactant. *Biomacromolecules, 8*, 708–712.

Yi, C., Xiaochen, S., Ying, C., Jian, G., Qi, C., & Xiqun, J. (2005). pH-induced self-assembly and capsules of sodium alginate. *Biomacromolecules, 6*, 2189–2196.